Journal of Electromyography and Kinesiology 33 (2017) 1–9

Contents lists available at ScienceDirect

Journal of Electromyography and Kinesiology

journal homepage: www.elsevier.com/locate/jelekin

Validation of a personalized curved muscle model of the lumbar spine during complex dynamic exertions

Jaejin Hwang, Gregory G. Knapik, Jonathan S. Dufour, Thomas M. Best [1], Safdar N. Khan [2], Ehud Mendel [3], William S. Marras *

Biodynamics Laboratory, Spine Research Institute, Department of Integrated Systems Engineering, The Ohio State University, 210 Baker Systems Engineering, 1971 Neil Avenue, Columbus, OH 43210, USA

ARTICLE INFO

Article history:
Received 30 July 2016
Received in revised form 5 January 2017
Accepted 6 January 2017

ABSTRACT

Previous curved muscle models have typically examined their robustness only under simple, single-plane static exertions. In addition, the empirical validation of curved muscle models through an entire lumbar spine has not been fully realized. The objective of this study was to empirically validate a personalized biologically-assisted curved muscle model during complex dynamic exertions. Twelve subjects performed a variety of complex lifting tasks as a function of load weight, load origin, and load height. Both a personalized curved muscle model as well as a straight-line muscle model were used to evaluate the model's fidelity and prediction of three-dimensional spine tissue loads under different lifting conditions. The curved muscle model showed better model performance and different spinal loading patterns through an entire lumbar spine compared to the straight-line muscle model. The curved muscle model generally showed good fidelity regardless of lifting condition. The majority of the 600 lifting tasks resulted in a coefficient of determination (R^2) greater than 0.8 with an average of 0.83, and the average absolute error less than 15% between measured and predicted dynamic spinal moments. As expected, increased load and asymmetry were generally found to significantly increase spinal loads, demonstrating the ability of the model to differentiate between experimental conditions. A curved muscle model would be useful to estimate precise spine tissue loads under realistic circumstances. This precise assessment tool could aid in understanding biomechanical causal pathways for low back pain.

1. Introduction

It is not currently possible to directly monitor spine tissue loads of human subjects during daily activities or occupational tasks, hence indirect validation approaches have been investigated. One approach uses biomechanical models, validation is important to evaluate how reliably these models estimate spine tissue loads under realistic circumstances. Various measures have been employed to assess the validity of these models.

Curved muscle models of the spine showed potential benefits compared to the straight-line muscle models (Kruidhof and Pandy, 2006; van Lopik and Acar, 2007; Vasavada et al., 2008). Curved muscle paths were generally designed by "via-point" and "obstacle-set" methods implemented in biomechanical models (Hwang et al., 2016d). The "via-point" let muscles connect through intermediate points along the muscle path, and it helped them flexibly coordinate with spinal movements in complex motions. The "obstacle-set" is an alternative way to allow muscles to wrap around predefined geometrical surfaces to generate curved muscles. These curved muscle paths improved the accuracy of muscle moment-arms, muscle forces, and joint moments compared to the straight-line muscle models (Arjmand et al., 2006; Kruidhof and Pandy, 2006; Vasavada et al., 2008).

Moment-generating capacity, muscle path deviation, compression spinal loads, and moment matching capability are important variables typically considered when examining the robustness of curved muscle models of the spine. Moment-generating capacity and compression spinal load of curved muscle models were generally compared with previous results of experimental studies or

* Corresponding author.
E-mail addresses: hwang.285@osu.edu (J. Hwang), knapik.1@osu.edu (G.G. Knapik), dufour.8@osu.edu (J.S. Dufour), Tom.Best@osumc.edu (T.M. Best), Safdar.Khan@osumc.edu (S.N. Khan), Ehud.Mendel@osumc.edu (E. Mendel), marras.1@osu.edu (W.S. Marras).
[1] Department of Family Medicine, The Ohio State University, Martha Morehouse Medical Plaza, 2050 Kenny Dr., Columbus, OH 43210, USA.
[2] Department of Orthopaedics, College of Medicine, The Ohio State University, Columbus, OH 43210, USA.
[3] Department of Neurological Surgery, The Ohio State University, Columbus, OH 43210, USA.

http://dx.doi.org/10.1016/j.jelekin.2017.01.001
1050-6411/

modeling studies (non-curved muscle), which are based on different subject groups and different exertions (Cholewicki and McGill, 1996; Han et al., 2012; van Lopik and Acar, 2007; Stokes et al., 2011; Vasavada et al., 1998). Even though these measures could evaluate if predicted values of curved muscle models were within the physiological range of previous results, the validation of a specific subject or a specific task was not possible.

The tasks used for evaluation are also important to assess if curved muscle models can accurately estimate spine tissue loads under realistic circumstances. For example, previous studies have examined curved muscle model performance under restricted conditions (static postures (Hajihosseinali et al., 2014; Han et al., 2012; Jaeger et al., 2012; van Lopik and Acar, 2007; Stokes et al., 2011; Suderman et al., 2012a; Suderman and Vasavada, 2012b; Vasavada et al., 1998), symmetric dynamic lifting (Van Dieen and Kingma, 2005), and occupational tasks (Cholewicki and McGill, 1996; Van Dieen and Kingma, 2005)). However, most tasks were performed in a pure single (cardinal) plane rather than in complex asymmetric exertion that simultaneously load multiple (combined) planes. For example, the static postures including the single plane-flexion, extension, axial rotation, lateral bending and upright postures were commonly tested for the examination of curved muscle spine models, whereas dynamic complex occupational tasks were seldom studied.

In addition, validation of the entire lumbar spine is essential to evaluate the accuracy of spine tissue loading through the entire lumbar spine. However, most biomechanical models have focused on the validation of a single disc level such as L3/L4 (Nussbaum and Chaffin, 1998), L4/L5 (Cholewicki and McGill, 1996; Arjmand et al., 2010), or L5/S1 (de Zee et al., 2007; Gagnon et al., 2001; Van Dieen and Kingma, 2005). If biomechanical models attempt to evaluate the spine tissue loads through the entire lumbar spine, the validation of various disc levels from T12/L1 through L5/S1 would improve the accuracy of spine tissue load estimations.

In sum, the empirical validations of curved muscle models of the entire lumbar spine are still not fully understood. In order to address this issue, our recently developed curved muscle model (Hwang et al., 2016b) was empirically tested for 12 subjects within a moderate motion range of lifting exertions (load asymmetry up to 60°, load weight up to 13.6 kg, and load height up to waist level) (Hwang et al., 2016c). It found that the curved muscle showed a robust model fidelity (mean $R^2 > 0.8$; mean AAE < 15%) and higher model performance than the straight-line muscle model of the lumbar spine. However, extreme ranges of physical lifting conditions that have been observed in occupational setting (Marras et al., 1993) have not been examined in terms of lumbar spine loading. In order to accurately evaluate the risk of low back injuries under these extreme loading yet realistic conditions, comprehensive validation approaches of the entire lumbar spine are necessary.

Thus, the objective of this study was to empirically investigate both model fidelity and prediction of spine tissue loads of the entire lumbar spine using the curved muscle model during extreme range of complex dynamic lifting tasks. In addition, predictions were compared to previous straight-line models.

2. Methods

2.1. Subjects

Twelve subjects (6 males and 6 females) participated in this study. Mean (standard deviation) age, body mass, and stature of males and females were summarized in Table 1, respectively. They did not have prior history of low back pain that resulted in the seeking of medical attention.

Table 1
Characteristics of the subjects analyzed in the study.

Gender	Age (years) Mean ± SD	Height (cm) Mean ± SD	Body mass (kg) Mean ± SD
Male	27.7 ± 6.3	175.8 ± 5.6	82.3 ± 11.5
Female	25.5 ± 4.2	169.7 ± 3.3	64.9 ± 8.8

2.2. Apparatus

Electromyographic (EMG) activity of 10 trunk muscles was collected with surface electrodes (Motion Lab Systems MA300-XVI, Baton Rouge, Louisiana, USA) with 1000 Hz sampling rate. Kinematic data of individual body segments and force plates was collected via a 24 camera Optitrack Flex 3 motion capture system (NaturalPoint, Corvallis, OR, USA) with 100 Hz sampling rate. The ground reaction forces and moments were recorded with a Bertec 4060A force plate (Bertec, Worthington, OH, USA) with 1000 Hz sampling rate. All signals were simultaneously gathered with customized laboratory software via a National Instruments USB-6225 data acquisition board (National Instruments, Austin, TX, USA).

2.3. Procedure

After arriving at the laboratory, subjects were informed about the general procedures of the experiment and signed a consent form approved by the University's Institutional Review Board.

Anthropometric measurements including body mass, stature, trunk circumference, trunk breath, and trunk depth were collected. After gentle skin abrasion and cleansing with alcohol, the surface electrodes (Ambu A/S, Ballerup, Denmark) with inter-electrode distance of approximately 3 cm were attached to 10 trunk muscles including the right and left latissimus dorsi (most lateral portion of the muscle at the T9 level), erector spinae (approximately 4 cm apart from midline of spine at the L3 level), rectus abdominis (3 cm from the midline of the abdomen, and 2 cm above the umbilicus), external obliques (10 cm from the midline of the abdomen and 4 cm above the ilium at 45° to the midline of the abdomen), and internal obliques (4 cm above ilium in the lumbar triangle at 45° to the midline of the spine) based on the standard placement guidelines (Mirka and Marras, 1993). The reference electrode was placed over the right anterior superior iliac crest. Forty-one reflective markers were placed on body segments and bony landmarks based on the baseline marker set in the OptiTrack's Motive optical motion capture software. For example, for the trunk, 3 markers were placed on the back (2 markers close to the lowest end of the scapular bone and 1 marker on the spine right below the neck) and 1 marker was on the chest (center of the sternum) of the torso. For the pelvis, 4 markers were located on the left/right anterior iliac spine bone and back of the waist (about 10 cm above the hip joint). The gross trunk angle measured was partitioned into multiple motion segments from T12/L1 through L5/S1 based on dynamic trunk angles and subject anthropometry according to regression models developed from a standing MRI database (Splittstoesser et al., 2011).

Subjects were instructed to perform calibration exertions to personalize muscle properties including the maximum muscle force per unit area, active and passive muscle force-length, and muscle force-velocity relationships in the model. These calibration exertions consisted of concentric and eccentric lumbar motions and exertions in multiple planes while holding a 9.1 kg weight. It encouraged various ranges of muscle length, muscle velocity, and muscle activities of each person, and this training data set was used to optimize personalized muscle properties. After calibration, subjects performed the lifting tasks as an independent data set. The

specific lifting tasks were not used in calibration exertions to minimize overfitting the data. Basic concentric and eccentric exertions in multiple planes were only employed in training data set (calibration) to optimize muscle properties that applicable in broader range of exertions rather than only lifting. Subjects lifted a box as a function of load weight (9.1 kg and 15.9 kg), load origin (counterclockwise 90°, counterclockwise 45°, 0°, clockwise 45°, and clockwise 90°), and load height (mid-calf, mid-thigh, and shoulder). Load height order was counterbalanced between subjects and all other conditions were completely randomized. In order to protect participants from risk of shoulder injuries, lifting from shoulder height was only conducted with a 9.1 kg load weight. A total of 50 lifting tasks were performed by each subject. Examples of calibration exertion and lifting task are described in Fig. 1.

2.4. Spine load assessment

A personalized biologically-assisted curved muscle model's structure was described previously (Hwang et al., 2016b). This model featured curved muscle lines of action generated from magnetic resonance imaging (MRI)-derived regression equations. The regression equations used anthropometric measures from each individual subject to predict personalized muscle moment-arms and physiological cross-sectional areas at various levels of the spine. The fidelity of this regression model was investigated in a previous study (Hwang et al., 2016a). The "via-point" technique was employed to allow muscles to coordinate with various movements of the spinal column. Each via-point was mechanically attached to each vertebral body, and individual muscle force was transmitted through these points. Muscle forces of latissimus dorsi, erector spinae, and rectus abdominis were acting through the muscle centroid path (Bogduk et al., 1998; Dumas et al., 1991; Stokes and Gardner-Morse, 1999), whereas muscle forces of external and internal obliques were transmitted through fiber-oriented paths (Dumas et al., 1991). In the curved muscle model, the total muscle force calculation was divided into active and passive muscle force whereas the straight-line muscle model accounted combined active and passive muscle force. A nonlinear constrained optimization technique was utilized to find suitable individual muscle properties (within physiological ranges) of each subject. The curved muscle model's objective function targeted to minimize average multi-planar root-mean-square error (RMSE) between internal and external moments of all lumbar disc levels. The straight-line muscle model's objective function was to minimize the RMSE at only L5/S1 level. The moment matching capabilities between the external and internal moments from T12/L1 through the L5/S1 level were used as validation measures. The internal spinal moments were summed for each muscle, which was the product between the muscle moment-arms and muscle forces. The external spinal moments of multiple disc levels were derived by measured ground reaction forces and torques via force plates, and the inertial moments of body segments. Trunk segment mass from T12 to L5 was estimated as a function of anthropometric measures (Bazrgari et al., 2008).

2.5. Data analysis

For the model fidelity measures, the multi-planar weighted squared correlation coefficient (R^2) and the multi-planar (sagittal and lateral planes) weighted average absolute error (AAE) were used. The R^2 indicated the amount of dynamic moment variability explained by comparing external and internal spinal moments. The AAE represented the magnitude of error between external and internal moments, and it was normalized by peak external moment of each trial. For the multi-planar weighted model fidelity measures, the summation of single-planar measures (sagittal and lateral planes) was weighted relative to peak in-plane external moments. This procedure gave more emphasis to the planes that supported greater loads. The robust of this measure was reported elsewhere (Dufour et al., 2013). The R^2 and AAE values were computed within each trial, and then these were averaged across trials within a given condition. For the spinal load assessments, the peak absolute three-dimensional spine tissue loads at the superior endplate of disc levels were evaluated.

2.6. Statistical analysis

The sample size was determined by the power analysis to detect a mean difference (with a significance level of 0.05) in three-dimensional spinal loads from T12/L1 through the L5/S1

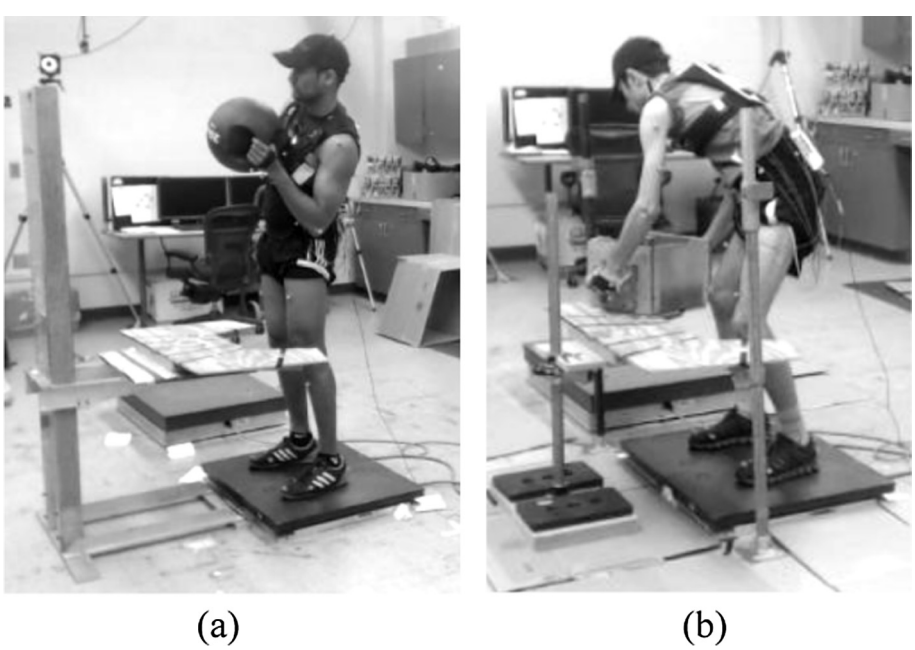

Fig. 1. Examples of the experimental set up for male subjects. (a) Calibration exertion. (b) Asymmetric lifting task.

levels between the curved muscle model and the straight-line muscle model. The medium effect size and power were set as 0.25 and 85%, respectively. The estimated minimum sample size was 12 subjects for within-subject ANOVA with repeated measures (G∗Power 3.1.9.2, Kiel University, Kiel, Germany).

Descriptive analysis was performed to summarize the overall mean and standard deviations of model fidelity measures. The statistical effects of various physical lifting conditions on the spinal loads of the curved muscle model were further analyzed using the Univariate analysis of variance (ANOVA) with a significance level 0.05. Load weight, load origin, and load height served as independent variables. The peak absolute three-dimensional spine tissue loads at each disc level served as dependent variables. Main effects and two-way interaction effects were analyzed, and subject was considered as a blocking factor.

3. Results

3.1. Model comparison

Fig. 2 shows the mean and standard deviations of weighted multi-planar R^2 and normalized AAE at each disc level between the curved and straight-line muscle models. The curved muscle model showed higher R^2 compared to the straight-line muscle model through the lumbar spine, and the biggest difference was 0.1. For the normalized AAE, curved muscle model showed up to 18% less AAE compared to the straight-line muscle model of an entire lumbar spine. Differences in model performance between two models were the greatest at the upper lumbar spine levels.

Fig. 3 depicts the comparison of the mean three-dimensional spinal loads between the curved and straight-line muscle models during lifting tasks. Curved muscle model showed higher compression up to 640 N compared to the straight-line muscle model. For the AP shear load, the curved muscle model showed lower values up to 575 N compared to the straight-line muscle model. For the lateral shear load, curved muscle model showed lower values relative to the straight-line muscle model except at the L5/S1 level, and the biggest difference (521 N) occurred at T12/L1 level. Similar to findings of the model fidelity, difference of three-dimensional loads between two models was the greatest at upper levels.

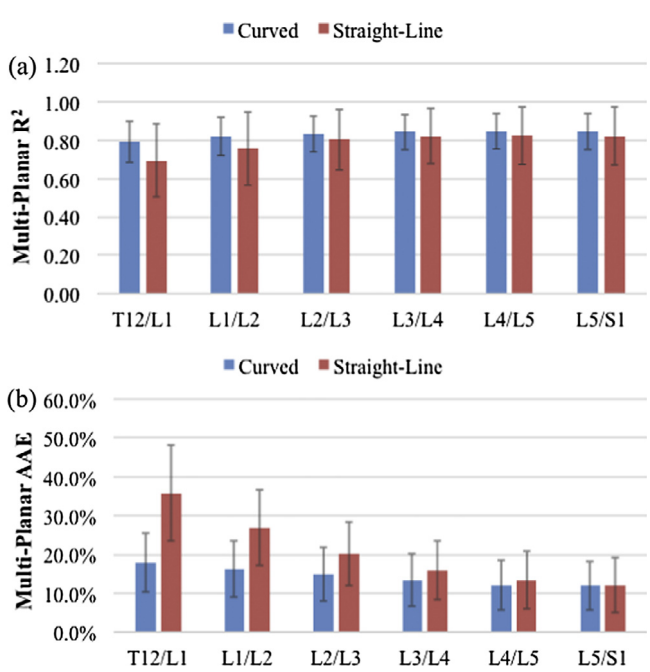

Fig. 2. Mean and standard deviations of the multi-planar R^2 (a) and normalized AAE (b) between curved and straight-line muscle models during complex lifting tasks.

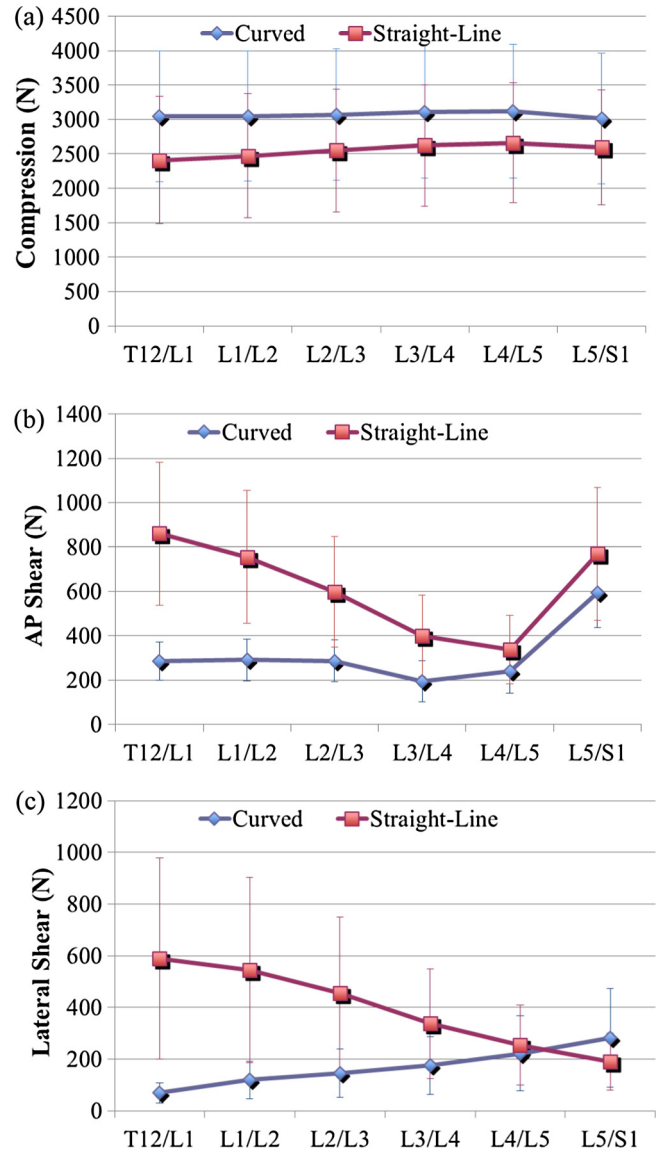

Fig. 3. Comparison of the mean and standard deviation of compression (a), AP shear (b), and Lateral shear (c) loads between the curved and straight-line muscle models during complex lifting tasks.

3.2. Model fidelity by lifting conditions

Figs. 4 and 5 show the mean and standard deviations of the R^2 and normalized AAE of the curved muscle model as a function of the load weight, load origin, and load height. The model generally demonstrated robust model fidelity across various physical lifting conditions (Figs. 4 and 5).

3.3. Spinal loads by lifting conditions

Table 2 shows a summary of statistical significant differences in three-dimensional peak spinal loads of the curved muscle model as a function of independent variable main effects and two-way interactions for all disc levels. Fig. 6 shows mean peak three-dimensional spinal loads as a function of the load weight, load origin, and load height, and biomechanically significant changes of

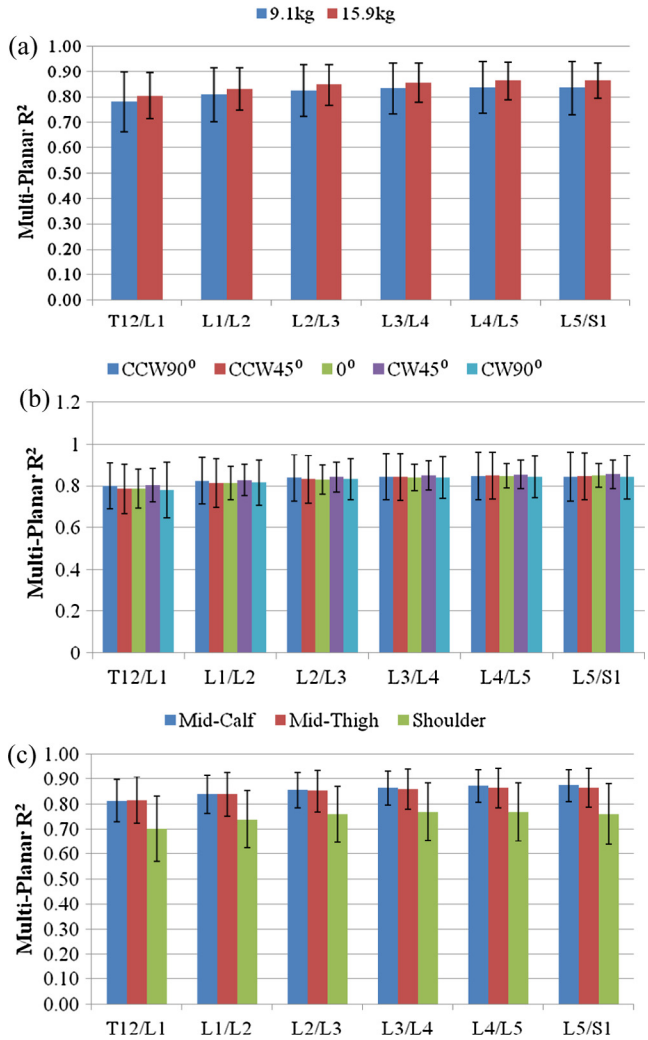

Fig. 4. Mean and standard deviation of multi-planar R^2 of the curved muscle model at the various levels as a function of load weight (a), load origin (b), and load height (c). CCW = counterclockwise; CW = clockwise.

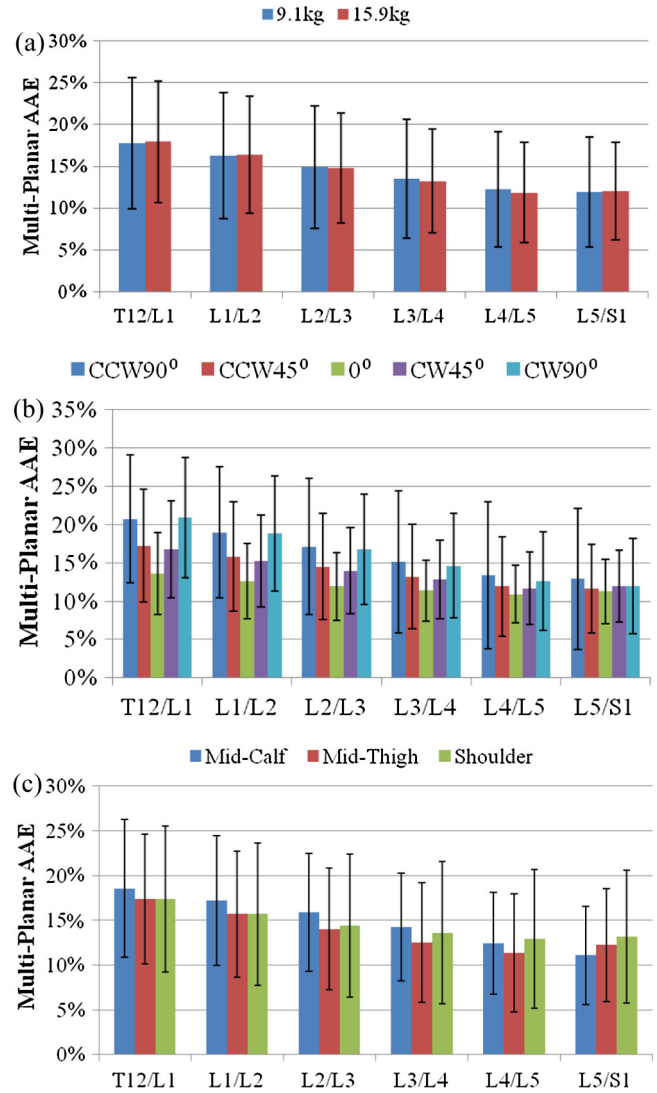

Fig. 5. Mean and standard deviation of multi-planar average absolute error (AAE) of the curved muscle model at the various levels as a function of load weight (a), load origin (b), and load height (c). CCW = counterclockwise; CW = clockwise.

spinal loads were only described here. The load weight showed significant differences in three-dimensional spinal loads for all levels. Lifting heavier weight increased the three-dimensional spinal loads. The load origin had significant effects on the anterior-posterior shear loads and lateral shear loads at most levels. For example, lifting from a more asymmetric origin increased the lateral shear loads at all levels (Fig. 6). Load height significantly influenced the compression and anterior-posterior shear loads at all levels. Lifting from lower height (relative to shoulder) increased compression (Fig. 6). Lifting from the lowest height (mid-calf) showed the highest anterior-posterior shear loads at L4/L5 and L5/S1, whereas the highest height (shoulder) caused the greatest anterior-posterior shear loads at upper levels (Fig. 6). The interaction between the load origin and the load height showed significant effects on the compression and anterior-posterior shear loads at most levels. For example, lifting from lower heights caused a greater increase in spine loading as the lifts became more asymmetric (Fig. 7).

4. Discussion

The present study showed that the personalized curved muscle model demonstrated higher model fidelity compared to the straight-line muscle model during extreme range of complex dynamic lifting tasks. The average resultant R^2 and AAE for all levels combined were 0.83 and 14.42%, respectively. This is the first known effort of an empirical validation study across multiple anatomical planes and multiple disc levels simultaneously for a biologically (EMG) driven biomechanical spine model during realistic complex dynamic lifting tasks. The model also demonstrated that its performance was generally not sensitive to the type of experimental condition being evaluated. Accordingly, the curved muscle model can reliably estimate three-dimensional spinal loads throughout extreme range of trunk motions during lifting exertions. In addition, this model was able to identify significant changes in spine tissue loads as a function of load weight, load origin, and load height during lifting tasks, hence indicating the model's utility to estimate precise spine tissue loads during complex dynamic lifting jobs.

The curved muscle model showed better model fidelity than the straight-line muscle model throughout the lumbar spine. Differences in model performance between two models increased as the more superior disc levels were considered. The curved muscle model showed robust model fidelity across the lumbar spine, whereas the straight-line muscle model showed worse performance at upper levels (Fig. 2). This trend was most likely a function

Table 2
Summary of statistically significant main effects and two-way interactions (*P*-values).

Measures	Disc levels	Load weight	Load origin	Load height	Load weight × Load origin	Load weight × Load height	Load origin × Load height
Peak compression (N)	T12/L1	<0.0001*	0.1539	<0.0001*	0.7098	0.7584	<0.0001*
	L1/L2	<0.0001*	0.1346	<0.0001*	0.7135	0.7835	<0.0001*
	L2/L3	<0.0001*	0.1418	<0.0001*	0.7083	0.7853	<0.0001*
	L3/L4	<0.0001*	0.1528	<0.0001*	0.6917	0.7835	<0.0001*
	L4/L5	<0.0001*	0.1548	<0.0001*	0.6806	0.7952	<0.0001*
	L5/S1	<0.0001*	0.1597	<0.0001*	0.6958	0.7898	<0.0001*
Peak AP shear (N)	T12/L1	<0.0001*	0.0001*	<0.0001*	0.4252	0.2574	0.0325*
	L1/L2	<0.0001*	<0.0001*	<0.0001*	0.3198	0.3768	0.0035*
	L2/L3	<0.0001*	0.0070*	<0.0001*	0.2243	0.8193	0.0652
	L3/L4	0.0021*	0.0815	0.0019*	0.3150	0.0136*	<0.0001*
	L4/L5	0.0331*	0.0011*	<0.0001*	0.0821	0.1908	<0.0001*
	L5/S1	0.0003*	0.0038*	<0.0001*	0.4483	0.7136	<0.0001*
Peak lateral shear (N)	T12/L1	0.0114*	<0.0001*	0.1251	0.1756	0.8284	0.0916
	L1/L2	0.0066*	<0.0001*	0.1329	0.5946	0.1864	0.0938
	L2/L3	0.0028*	<0.0001*	0.0919	0.4105	0.1036	0.0755
	L3/L4	0.0018*	<0.0001*	0.0535	0.1586	0.0779	0.0461*
	L4/L5	0.0008*	<0.0001*	0.0051*	0.0775	0.0789	0.0020*
	L5/S1	0.0003*	<0.0001*	0.0004*	0.0451*	0.1051	<0.0001*

* Indicated *P*-values < 0.05. AP = Anterior-posterior.

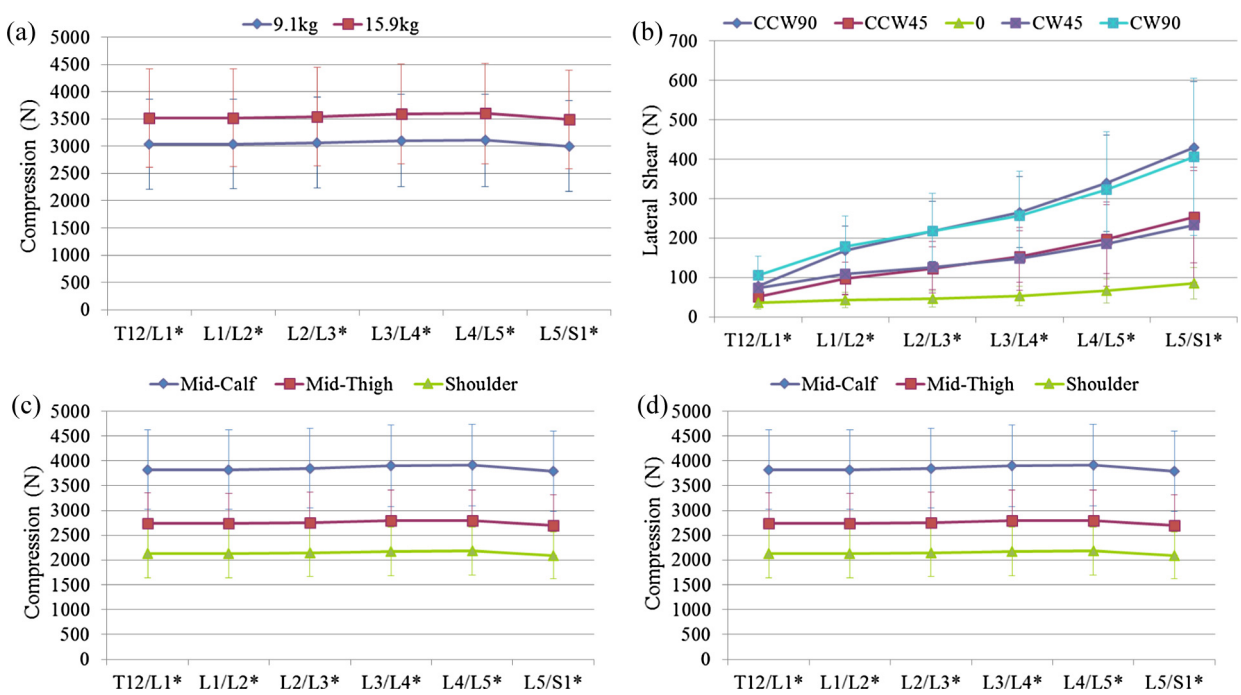

Fig. 6. Mean and standard deviation of compression at the various levels as a function of the load weight (a), lateral shear load by load origin (b), compression by load height (c), and AP shear by load height (d). * Indicates the significant difference between levels, $P < 0.05$. CCW = counterclockwise; CW = clockwise; AP = anterior-posterior. Only biomechanically significant changes of spinal loads were included in this figure.

of the fact that muscles start displaying increased curvatures at upper levels which resulted in significantly different spinal load distributions (especially in AP shear and lateral shear loads) between two models (Fig. 3). In curved muscle model, erector spinae (major power producing muscle) was more longitudinally aligned with the lumbar spine curvature compared to the straight-line muscle model. It might cause the curved muscle model generally showed higher compression and lower shear loads than the straight-line muscle model. Based upon better model fidelity of the curved muscle model compared to the straight-line muscle model, the present study confirms the advantages of the curved muscle approach.

Our previous validation paper (Hwang et al., 2016c) compared the performance of the straight-line muscle model under conditions where the straight-line muscle model was known to work reasonably well (Granata and Marras, 1995; Marras and Granata, 1997; Theado et al., 2007) to show what improvement was possible. The current paper was intended to push the model to the limits and explore extreme lifting postures that are not typically evaluated by biomechanical models. In terms of the load weight, the revised NIOSH lifting equation (1993) recommend maximum lifting loads up to approximately 23 kg under ideal lifting conditions (Waters et al., 1993). Since present study employed complex lifting conditions with extreme range of load height and load origins rather than optimal symmetric lifting conditions, 15.9 kg load weight was empirically found as a maximum load limit to subjects in pilot study. The comparison of the model fidelity between the previous and present validation studies was conducted. Table 3

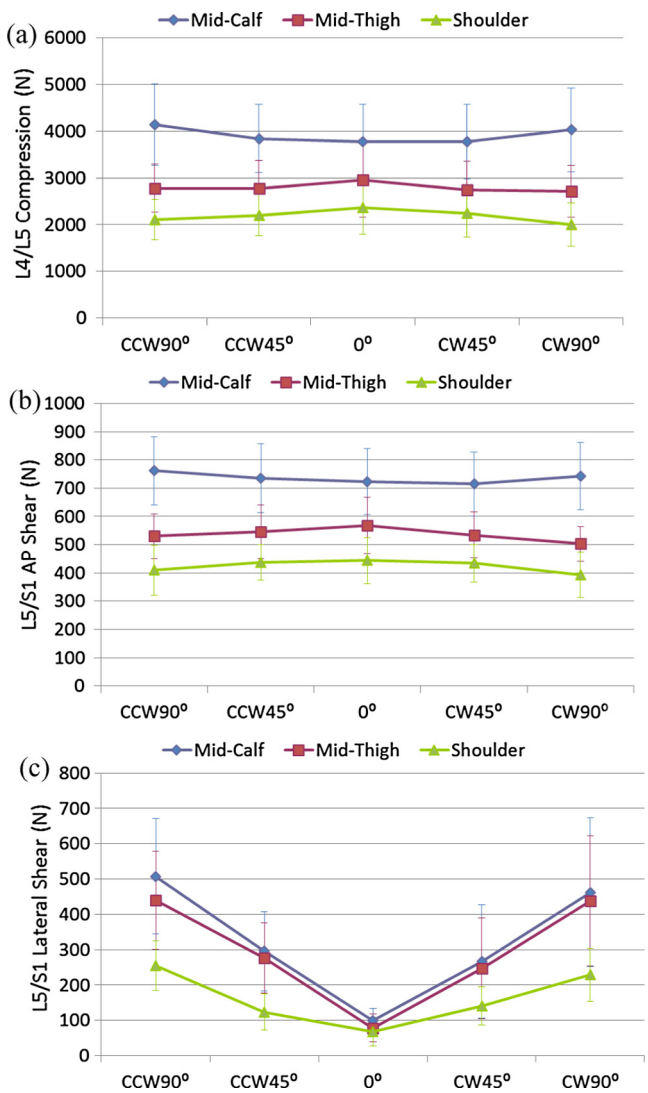

Fig. 7. The interaction effect between the load origin and load height on the peak three-dimensional spine tissue loads at each disc level which had highest spinal loads (mean ± SD). CCW = counterclockwise; CW = clockwise; AP = anterior-posterior.

shows the total average multi-planar R^2 and normalized AAE across all levels of two studies that used different subject groups, respectively. The present study generally showed a comparable model performance with a previous study. It indicated that the curved muscle model provides reliable spinal load estimations up to extreme range of lifting tasks.

Model performance was generally not dependent on experimental conditions. However, lifting from shoulder height yielded slightly lower multi-planar R^2s at all spine levels compared to lifting from other heights, with a mean difference around 0.1 (Fig. 4). The lifting from shoulder height required minimal lumbar motion but substantial muscle activations which was different from the characteristics of the training data set (calibrations) that encouraged a wider range of lumbar motions with substantial muscle activations. Thus, optimized muscle parameters based on the calibration exertions could not effectively cover the muscle activations with minimal change of muscle lengths. This issue could be improved by adding the isometric types of exertions in calibration training data set.

The only other experimental condition that decreased the model performance was lifting from extreme asymmetries. Lifting from extreme asymmetric origins slightly increased the multi-planar normalized AAE of the upper levels of the lumbar spine (Fig. 5). During asymmetric lifting in particular, lateral moments tended to be overestimated in the upper levels, which was partially related to the high lateral moment contribution of the latissimus dorsi. This latissimus dorsi's overestimation at upper levels could be associated with slightly worse overall model performance of upper levels compared to lower levels in the curved muscle model. This overestimation issue could be partially explained by the activation of latissimus dorsi that was primarily driven by moments at the shoulder rather than the moments at the low back. Furthermore, the limited range of calibration exertions, which only optimized for a moderate range of the length of the latissimus dorsi, could affect the result. These under/over-estimation issues could be improved with calibration exertions that cover a wider range of eccentric and concentric exertions.

The variation in spine tissue loads as a function of load weight, load origin, and load height were similar to previous findings (Davis and Marras, 2000; Dufour et al., 2013; Granata and Marras, 1999; Hwang et al., 2016c; Jorgensen et al., 1999; Marras et al., 2003; Marras and Sommerich, 1991). As expected, lifting heavier objects required the recruitment of greater muscles forces to counterbalance larger external loads, therefore resulting in increased three-dimensional spinal loads as reported in previous studies (Davis and Marras, 2000; Hwang et al., 2016c; Marras et al., 2003; Marras and Sommerich, 1991). Peak lateral shear loads significantly increased as subjects lifted from more asymmetric origins (Fig. 6). During asymmetric lifting, the left/right side of the extensor muscles were highly activated to counterbalance lateral moments (Granata and Marras, 1999), resulting in greater lateral shear loads as noted previously (Davis and Marras, 2005; Granata and Marras, 1999; Hwang et al., 2016c). These findings

Table 3
Comparison of the curved muscle model performance with a previous study.

	Hwang et al. (2016c)			Present study		
Variables	Levels	R^2	AAE (%)	Levels	R^2	AAE (%)
Load weight	6.8 kg	0.83	13.51	9.1 kg	0.86	14.41
	13.6 kg	0.84	13.09	15.9 kg	0.84	14.37
Load origin	CCW 60°	0.85	13.79	CCW 90°	0.83	14.91
	CCW 30°	0.84	13.00	CCW 45°	0.83	14.06
	0°	0.82	13.00	0°	0.83	11.96
	CW 30°	0.84	13.00	CW 45°	0.84	13.74
	CW 60°	0.84	13.86	CW 90°	0.83	15.96
Load height	Ankle	0.80	13.93	Mid-calf	0.85	14.91
	Knee	0.86	12.95	Mid-thigh	0.85	13.87
	Waist	0.83	13.52	Shoulder	0.75	14.54

Note: Average multi-planar R^2 and normalized AAE (%) of all levels were reported.

further validate the ability of the model to functionally differentiate the effects of muscle recruitment patterns, kinematics, and kinetics on loading of spinal tissues during complex working conditions.

The anterior-posterior shear loads at L4/L5 and L5/S1 were highest when subject lifted from mid-calf height, whereas the highest anterior-posterior shear load existed in upper levels (from T12/L1 to L2/L3) when lifting from shoulder height (Fig. 6). This result was highly associated with the curvature of the lumbar spine during each condition. For instance, L4/L5 and L5/S1 were anatomically positioned more horizontally than the upper levels in upright postures, so higher anterior-posterior shear loads at upper levels compared to L4/L5 and L5/S1 were observed as in previous studies (Knapik and Marras, 2009; Marras et al., 2009).

The interaction between load origin and load height significantly affected three-dimensional spine tissue loads (Fig. 7). Lifting from the lowest height (mid-calf) and the most asymmetric origin (90°) produced the highest loads, which confirmed the results of a previous study (Davis and Marras, 2005; Hwang et al., 2016c). An epidemiologic study reported that the risk for low back disorders was increased in jobs that required frequent asymmetric or twisting postures (Ferguson et al., 2004; Marras et al., 1993; Punnett et al., 1991). The interaction plot from the current study provides insight as to how this risk for back injuries sustained during asymmetric postures could be exacerbated at lower heights (Fig. 7).

Several potential limitations should be noted when interpreting the results of this study. First, this model was only empirically tested during complex dynamic lifting exertions. However, the empirical validation of other occupational tasks such as pushing, pulling, lowering, and carrying exertions would also be expected to enhance the accuracy of spine tissue load estimations during complex tasks. Second, this model was only investigated for young healthy subject group (mean age = 26.6 years). An elderly subject group or low back patient group might have different muscle recruitment patterns during complex lifting tasks (Marras et al., 2004), which could affect model performance and spine tissue loads. Lastly, the under/over-estimations of spinal moment predictions might be related to the range of calibration exertions optimized. Application of a wider set of calibration exertions would likely improve the model's performance and predictive capabilities.

In conclusion, the personalized curved muscle model evaluated in this study was empirically tested during extreme ranges of dynamic lifting conditions and demonstrated better model fidelity than the straight-line muscle model. The model's robust performance indicated that the curved muscle representations were biomechanically and physiologically reasonable, and would provide additional insights of the complex load distributions of an entire lumbar spine compared to the straight-line muscle model. This model can now be used to more accurately assess the spinal loads during complex occupational exertions, and will help improve our ability to prevent low back disorders by further understanding biomechanical causal pathways.

References

Arjmand, N., Gagnon, D., Plamondon, A., Shirazi-Adl, A., Larivière, C., 2010. A comparative study of two trunk biomechanical models under symmetric and asymmetric loadings. J. Biomech. 43, 485–491.

Arjmand, N., Shirazi-Adl, A., Bazrgari, B., 2006. Wrapping of trunk thoracic extensor muscles influences muscle forces and spinal loads in lifting tasks. Clin. Biomech. 21, 668–675.

Bazrgari, B., Shirazi-Adl, A., Kasra, M., 2008. Seated whole body vibrations with high-magnitude accelerations–relative roles of inertia and muscle forces. J. Biomech. 41, 2639–2646.

Bogduk, N., Johnson, G., Spalding, D., 1998. The morphology and biomechanics of latissimus dorsi. Clin. Biomech. 13, 377–385.

Cholewicki, J., McGill, S.M., 1996. Mechanical stability of the in vivo lumbar spine: implications for injury and chronic low back pain. Clin. Biomech. 11, 1–15.

Davis, K.G., Marras, W.S., 2000. Assessment of the relationship between box weight and trunk kinematics: does a reduction in box weight necessarily correspond to a decrease in spinal loading? Hum. Factors 42, 195–208.

Davis, K., Marras, W.S., 2005. Load spatial pathway and spine loading: how does lift origin and destination influence low back response? Ergonomics 48, 1031–1046.

de Zee, M., Hansen, L., Wong, C., Rasmussen, J., Simonsen, E.B., 2007. A generic detailed rigid-body lumbar spine model. J. Biomech. 40, 1219–1227.

Dufour, J.S., Marras, W.S., Knapik, G.G., 2013. An EMG-assisted model calibration technique that does not require MVCs. J. Electromyogr. Kinesiol. 23, 608–613.

Dumas, G.A., Poulin, M.J., Roy, B., Gagnon, M., Jovanovic, M., 1991. Orientation and moment arms of some trunk muscles. Spine 16, 293–303.

Ferguson, S.A., Marras, W.S., Burr, D.L., Davis, K.G., Gupta, P., 2004. Differences in motor recruitment and resulting kinematics between low back pain patients and asymptomatic participants during lifting exertions. Clin. Biomech. 19, 992–999.

Gagnon, D., Larivière, C., Loisel, P., 2001. Comparative ability of EMG, optimization, and hybrid modelling approaches to predict trunk muscle forces and lumbar spine loading during dynamic sagittal plane lifting. Clin. Biomech. 16, 359–372.

Granata, K.P., Marras, W.S., 1995. An EMG-assisted model of trunk loading during free dynamic lifting. J. Biomech. 28, 1309–1317.

Granata, K.P., Marras, W.S., 1999. Relation between spinal load factors and the high-risk probability of occupational low-back disorder. Ergonomics 42, 1187–1199.

Hajihosseinali, M., Arjmand, N., Shirazi-Adl, A., Farahmand, F., Ghiasi, M.S., 2014. A novel stability and kinematics-driven trunk biomechanical model to estimate muscle and spinal forces. Med. Eng. Phys. 36, 1296–1304.

Han, K.-S., Zander, T., Taylor, W.R., Rohlmann, A., 2012. An enhanced and validated generic thoraco-lumbar spine model for prediction of muscle forces. Med. Eng. Phys. 34, 709–716.

Hwang, J., Dufour, J.S., Knapik, G.G., Best, T.M., Khan, S.N., Mendel, E., et al., 2016a. Prediction of magnetic resonance imaging-derived trunk muscle geometry with application to spine biomechanical modeling. Clin. Biomech. 37, 60–64.

Hwang, J., Knapik, G.G., Dufour, J.S., Aurand, A., Best, T.M., Khan, S.N., et al., 2016b. A biologically-assisted curved muscle model of the lumbar spine: model structure. Clin. Biomech. 37, 53–59.

Hwang, J., Knapik, G.G., Dufour, J.S., Best, T.M., Khan, S.N., Mendel, E., et al., 2016c. A biologically-assisted curved muscle model of the lumbar spine: model validation. Clin. Biomech. 37, 153–159.

Hwang, J., Knapik, G.G., Dufour, J.S., Marras, W.S., 2016d. Curved muscles in biomechanical models of the spine: a systematic literature review. Ergonomics. http://dx.doi.org/10.1080/00140139.2016.1190410.

Jaeger, R., Mauch, F., Markert, B., 2012. The muscle line of action in current models of the human cervical spine: a comparison with in vivo MRI data. Comput. Methods Biomech. Biomed. Eng. 15, 953–961.

Jorgensen, M.J., Davis, K.G., Kirking, B.C., Lewis, K.E., Marras, W.S., 1999. Significance of biomechanical and physiological variables during the determination of maximum acceptable weight of lift. Ergonomics 42, 1216–1232.

Knapik, G.G., Marras, W.S., 2009. Spine loading at different lumbar levels during pushing and pulling. Ergonomics 52, 60–70.

Kruidhof, J., Pandy, M.G., 2006. Effect of muscle wrapping on model estimates of neck muscle strength. Comput. Methods Biomech. Biomed. Eng. 9, 343–352.

van Lopik, D.W., Acar, M., 2007. Development of a multi-body computational model of human head and neck. Proc. Inst. Mech. Eng. Part K J. Multi-Body Dyn. 221, 175–197.

Marras, W.S., Davis, K.G., Jorgensen, M., 2003. Gender influences on spine loads during complex lifting. Spine J. 3, 93–99.

Marras, W.S., Ferguson, S.A., Burr, D., Davis, K.G., Gupta, P., 2004. Spine loading in patients with low back pain during asymmetric lifting exertions. Spine J. 4, 64–75.

Marras, W.S., Granata, K.P., 1997. The development of an EMG-assisted model to assess spine loading during whole-body free-dynamic lifting. J. Electromyogr. Kinesiol. 7, 259–268.

Marras, W.S., Knapik, G.G., Ferguson, S., 2009. Loading along the lumbar spine as influence by speed, control, load magnitude, and handle height during pushing. Clin. Biomech. 24, 155–163.

Marras, W.S., Lavender, S.A., Leurgans, S.E., Rajulu, S.L., Allread, W.G., Fathallah, F.A., et al., 1993. The role of dynamic three-dimensional trunk motion in occupationally-related low back disorders: the effects of workplace factors, trunk position, and trunk motion characteristics on risk of injury. Spine 18, 617–628.

Marras, W.S., Sommerich, C.M., 1991. A three-dimensional motion model of loads on the lumbar spine: II. Model validation. Hum. Fact. 33, 139–149.

Mirka, G.A., Marras, W.S., 1993. A stochastic model of trunk muscle coactivation during trunk bending. Spine 18, 1396–1409.

Nussbaum, M.A., Chaffin, D.B., 1998. Lumbar muscle force estimation using a subject-invariant 5-parameter EMG-based model. J. Biomech. 31, 667–672.

Punnett, L., Fine, L.J., Keyserling, W.M., Herrin, G.D., Chaffin, D.B., 1991. Back disorders and nonneutral trunk postures of automobile assembly workers. Scand. J. Work Environ. Health 17, 337–346.

Splittstoesser, R.E., Knapik, G.G., Marras, W.S., 2011. A simple model of changes in lumbar intervertebral angles during sagittal torso flexion. Proc. Human Fact. Ergon. Soc. Annu. Meet. 55, 1029–1033.

Suderman, B.L., Krishnamoorthy, B., Vasavada, A.N., 2012a. Neck muscle paths and moment arms are significantly affected by wrapping surface parameters. Comput. Methods Biomech. Biomed. Eng. 15, 735–744.

Suderman, B.L., Vasavada, A.N., 2012b. Moving muscle points provide accurate curved muscle paths in a model of the cervical spine. J. Biomech. 45, 400–404.
Stokes, I.A.F., Gardner-Morse, M.G., 1999. Quantitative anatomy of the lumbar musculature. J. Biomech. 32, 311–316.
Stokes, I.A.F., Gardner-Morse, M.G., Henry, S.M., 2011. Abdominal muscle activation increases lumbar spinal stability: analysis of contributions of different muscle groups. Clin. Biomech. 26, 797–803.
Theado, E.W., Knapik, G.G., Marras, W.S., 2007. Modification of an EMG-assisted biomechanical model for pushing and pulling. Int. J. Ind. Ergon. 37, 825–831.
Van Dieen, J.H., Kingma, I., 2005. Effects of antagonistic co-contraction on differences between electromyography based and optimization based estimates of spinal forces. Ergonomics 48, 411–426.
Vasavada, A.N., Li, S., Delp, S.L., 1998. Influence of muscle morphometry and moment arms on the moment-generating capacity of human neck muscles. Spine 23, 412–422.
Vasavada, A.N., Lasher, R.A., Meyer, T.E., Lin, D.C., 2008. Defining and evaluating wrapping surfaces for MRI-derived spinal muscle paths. J. Biomech. 41, 1450–1457.
Waters, T.R., Putz-Anderson, V., Garg, A., Fine, L.J., 1993. Revised NIOSH equation for the design and evaluation of manual lifting tasks. Ergonomics 36, 749–776.

Jaejin Hwang is an assistant professor in industrial and systems engineering department at Northern Illinois University. He received a Ph.D. in Industrial and Systems Engineering from the Ohio State University in 2016. His research area includes biomechanical modeling, exposure assessment, ergonomics intervention, and workplace wellness. His findings have been published over 20 peer-reviewed journal articles and conference proceeding papers.